Down-Regulation of Cell Surface Receptors Is Modulated by Polar Residues within the Transmembrane Domain

Lolita Zaliauskiene,*[†] Sunghyun Kang,*[†] Christie G. Brouillette,[‡] Jacob Lebowitz,[§] Ramin B. Arani,[||] and James F. Collawn*[◆]

*Departments of Cell Biology, [‡]Biochemistry and Molecular Genetics, and [§]Microbiology; and [||]Biostatistics Unit, Comprehensive Cancer Center, University of Alabama at Birmingham, Birmingham, AL 35294-0005

How recycling receptors are segregated from down-regulated receptors in the endosome is unknown. In previous studies, we demonstrated that substitutions in the transferrin receptor (TR) transmembrane domain (TM) convert the protein from an efficiently recycling receptor to one that is rapidly down regulated. In this study, we demonstrate that the "signal" within the TM necessary and sufficient for down-regulation is Thr[11]Gln[17]Thr[19] (numbering in TM). Transplantation of these polar residues into the wild-type TR promotes receptor down-regulation that can be demonstrated by changes in protein half-life and in receptor recycling. Surprisingly, this modification dramatically increases the TR internalization rate as well (~79% increase). Sucrose gradient centrifugation and cross-linking studies reveal that propensity of the receptors to self-associate correlates with down-regulation. Interestingly, a number of cell surface proteins that contain TM polar residues are known to be efficiently down-regulated, whereas recycling receptors for low-density lipoprotein and transferrin conspicuously lack these residues. Our data, therefore, suggest a simple model in which specific residues within the TM sequences dramatically influence the fate of membrane proteins after endocytosis, providing an alternative signal for down-regulation of receptor complexes to the well-characterized cytoplasmic tail targeting signals.

INTRODUCTION

Endocytosis is required for delivery of extracellular nutrients, down-regulation of growth factor receptors, and maintenance of cell polarity and membrane homeostasis (for review, see Mellman, 1996; Mukherjee *et al.*, 1997). After internalization, transport receptors such as the transferrin receptor (TR) deliver and release their cargo into the low-pH environment of the early endosome before recycling back to the cell surface (Dautry-Varsat *et al.*, 1983; Hopkins, 1983; Klausner *et al.*, 1983). Because the $t_{1/2}$ for TR recycling is ~16 min (Mukherjee *et al.*, 1997) and the TR protein half-life is >24 h (Omary and Trowbridge, 1981), the TR effectively serves as the prototype for a recycling receptor. Growth factor receptors, however, such as epidermal growth factor receptor, internalize after ligand binding and are rapidly delivered to lysosomes where they are degraded (Carpenter and Cohen, 1976;

Dunn *et al.*, 1986). Segregation of recycling and down-regulated receptors appears to occur at the level of the sorting endosome (for review, see Mukherjee *et al.*, 1997), with recycling receptors trafficking to the recycling endosome (Willingham *et al.*, 1984) before returning to the cell surface.

A number of studies suggest that lysosomal targeting is signal-mediated, whereas recycling occurs by default (for review, see Gruenberg and Maxfield, 1995). Perhaps the clearest example of this is the epidermal growth factor receptor that requires an active cytoplasmic kinase domain for entry into internal vesicles of the multivesicular body (Futter *et al.*, 1993). Other late endosomal/lysosomal targeting signals have been identified in the cytoplasmic tails of P-selectin (Green *et al.*, 1994), the mannose-6-phosphate receptor (Johnson and Kornfeld, 1992a,b), the major histocompatibility complex (MHC) class II invariant chain (Ii) (Bakke and Dobberstein, 1990; Pieters *et al.*, 1993; Bremnes *et al.*, 1994; Odorizzi *et al.*, 1994; Pond *et al.*, 1995; Kang *et al.*, 1998), the T cell receptor CD3 γ-chain (Letourneur and Klausner, 1992), lysosomal acid phosphatase (Peters *et al.*, 1990), and lysosome-associated membrane glycoprotein (Williams and Fukuda, 1990), suggesting that entry into multivesicular bodies does not occur by default.

Studies to determine the structural requirements for recycling have remained unsuccessful. For the TR, removal of the cytoplasmic tail (Jing *et al.*, 1990; Johnson *et al.*, 1993) or the extracellular domain (Rutledge *et al.*, 1991) has no effect on recycling or protein turnover. Furthermore, the kinetics of TR recycling is the same as the kinetics of lipid recycling, suggesting that recycling occurs as a constitutive, bulk flow process (Mayor *et al.*, 1993). A critical unanswered question, however, is what is the mechanism that distinguishes recycling receptors from down-regulated receptors in the sorting endosome? Clearly, one mechanism for down-regulation is by receptor cross-linking with multivalent ligands (Mellman and Plutner, 1984; Weissman *et al.*, 1986), but how this relates to the normal clearance process is unclear.

In previous studies, we demonstrated that a 10-residue region within the MHC class II Ii transmembrane domain (TM), when substituted for the corresponding region of the TR resulted in down-regulation of the TR mutant. In this study, we tested the role of polar residues within this region and demonstrated that three polar residues were necessary and sufficient to promote TR down-regulation. Surprisingly, inclusion of these residues also enhances TR endocytosis. Together, our studies suggest that the presence or absence of polar residues in the TM can dramatically alter the fate of the membrane proteins after endocytosis.

MATERIALS AND METHODS

Cells and Reagents

Chicken embryo fibroblasts (CEFs) were grown in DMEM supplemented with 1% chicken serum and 1% fetal bovine serum (Atlanta Biologicals, Norcross, GA), 2% (vol/vol) tryptose phosphate broth (Difco, Detroit, MI), 2 mM L-glutamine, penicillin, and streptomycin. Protease inhibitors (complete mini-inhibitors) were obtained from Roche Diagnostic (Indianapolis, IN).

Construction of TR and Ii-TR Chimera Transmembrane Mutants

Mutants were prepared as described previously (Odorizzi *et al.*, 1994) by the method of Kunkel (1985). The Ii_{TM} 11–19 mutant was originally described in Kang *et al.* (1998). The oligonucleotide primer for preparation of the Ii_{TM} 11–19 mutant was GGGACTATT<u>GC</u>-CCTGCTCCTCGCTGGC<u>GC</u>GGCC<u>GC</u>CTTTATGATTGGC, and the primer for the TR_{TM} $Thr^{11}Gln^{17}Thr^{19}$ mutant was GGGACTAT-T<u>AC</u>TGTGATCGTCTTTTT<u>CC</u>A<u>G</u>ATTA<u>C</u>ATTTATGATTGGC. The underlined bases indicate where the substitutions were introduced. All mutations were verified by dideoxynucleotide sequencing of the entire cytoplasmic and TMs in the expression vector BH-RCAS (Sanger *et al.*, 1977; Tabor and Richardson, 1987).

Expression of Ii and TR Mutants: Metabolic Labeling and Immunoprecipitation

Human TR and Ii-TR mutants were expressed in CEFs as described previously (Odorizzi *et al.*, 1994) by using the BH-RCAS expression vector. Metabolic labeling and Immunoprecipitation of CEFs expressing the various TR and Ii-TR constructs were performed as described previously (Odorizzi *et al.*, 1994).

Indirect Immunofluorescence

Double-label indirect immunofluorescence was performed as described previously (Odorizzi *et al.*, 1994). Slides were analyzed on an Olympus IX70 epifluorescence microscope. Optical sections were captured with a charge-coupled device, high-resolution camera equipped with a camera/computer interface. Images were analyzed with a Power Mac 9500/132 computer with IPLab Spectrum software (Scanalytics, Fairfax, VA).

Measurement of Transferrin (Tf) Internalization and Proteolysis

The rate of Tf internalization was determined with the internal surface (IN/SUR) method (Wiley and Cunningham, 1982) as described previously (Kang *et al.*, 1998). For the proteolysis assay, CEFs expressing the various TR and Ii-TR constructs were plated in triplicate at a density of 7.5×10^4 cells/cm², in 24-well tissue culture plates 24 h before the assay (Costar, Cambridge, MA). Cells were incubated in serum-free DMEM for 1 h at 37°C, and then washed once with ice-cold 0.15 M NaCl, 0.01 M sodium phosphate buffer (pH 7.4) containing 0.1% bovine serum albumin (BSA-PBS). The cells were then pulsed for 10 min at 37°C with ¹²⁵I-labeled Tf (4 μg/ml) in 0.15 ml of BSA-PBS. The medium was then removed, and the cells were washed three times with ice-cold BSA-PBS and incubated at 37°C with prewarmed (37°C) DMEM containing 0.1% BSA and 50 μg/ml unlabeled Tf for 0, 15, 30, 60, and 120 min. After incubation, the medium was collected, protein was precipitated in 10% trichloroacetic acid (TCA) and removed by centrifugation, and the acid-soluble and acid-insoluble radioactivity was counted in a gamma counter. The surface-bound and internalized Tf in CEFs was determined by the acid wash procedure described in Kang *et al.* (1998).

Tf Cross-linking

Aggregated Tf was prepared by reacting Tf (30 mg/ml) with a 20-fold molar excess of glutaraldehyde (Sigma, St. Louis, MO) in 50 mM PBS, pH 7.4, for 1 h at room temperature with gentle mixing. The reaction was quenched with the addition of lysine (to a final concentration of 0.1 M). The product was purified by gel filtration chromatography to separate the fractions into various MW ranges before ¹²⁵I-labeling. Fractions corresponding to Tf dimers (MW ~160 kDa) were radiolabeled and used for the proteolysis assay.

Sucrose Gradient Sedimentation

Oligomerization of the wild-type TR and Ii-TR chimeras was analyzed by velocity gradient centrifugation in sucrose performed essentially as described (Weisz *et al.*, 1993). Discontinuous 5–25% (wt/wt) sucrose gradients were poured over a 60% (wt/wt) sucrose cushion (0.35 ml) in SW50.1 tubes. The sucrose percentage difference between fractions was 2%. All solutions were in MNT buffer [100 mM NaCl, 20 mM Tris, 30 mM 2-(N-morpholino)ethanesulfonic acid, pH 5.8] containing 0.1% Triton X-100 and protease inhibitors. CEFs expressing wild-type TR, TR_{TM} $Thr^{11}Gln^{17}Thr^{19}$, Ii_{TM} 11–19, and Ii_{TM} 11–19 $Ala^{11}Ala^{17}Ala^{19}$ chimeras were metabolically labeled for 2 h and chased for 1 h in complete media. Cells were lysed in MNT buffer containing 1% Triton X-100 and protease inhibitors. Lysates were centrifuged at 38,000 rpm in a NVT90 rotor in Beckman ultracentrifuge for 30 min at 4°C. The supernatants were immediately loaded on the top of preformed sucrose gradients and centrifuged at 40,000 rpm in a SW50.1 rotor for 16 h at 4°C. Fractions (350 μl) were collected, immunoprecipitated with B3/25 antibody at pH 7, and analyzed on SDS-polyacrylamide gels. Immunoprecipitates were quantitated on a model 425 PhosphorImager (Molecular Dynamics, Sunnyvale, CA). The locations of the proteins in the gradient were compared with the protein standards, aldolase (7.4S), catalase (11.3S), and thyroglobulin (19.3S), which were centrifuged under the same conditions. The S values for the various constructs were calculated according to Martin and Ames (1961).

Receptor Cross-linking

CEF cells in 10-cm dishes expressing wild-type and mutant TRs were metabolically labeled with 1.2 mCi/ml *trans*-^{35}S label overnight and chased in complete media for 1 h. Cells were lysed in 50 mM HEPES-NaOH in lysis buffer (1% Triton X-100, 0.5% sodium deoxycholate, 0.3 M NaCl, pH 7.4) for 20 min. The postnuclear supernatants were incubated at room temperature with 1 mM 3,3′-dithiobis[sulfosuccinimidylpropionate] (DTSSP) (Pierce, Rockford, IL) for 20 min, and the reaction was stopped with an equal volume of 50 mM Tris-HCl in lysis buffer. Cross-linked samples were immunoprecipitated with B3/25 monoclonal antibody. The samples were then split into two fractions containing SDS sample buffer with reductant and without reductant. The immunoprecipitates were then analyzed by SDS-PAGE to evaluate the extent of cross-linking. Noncross-linked controls were analyzed to determine the position of a receptor dimer.

Calculation of Protein Half-Life

Down-regulation of membrane proteins from the cell surface can be represented by a two-compartment model, as illustrated below.
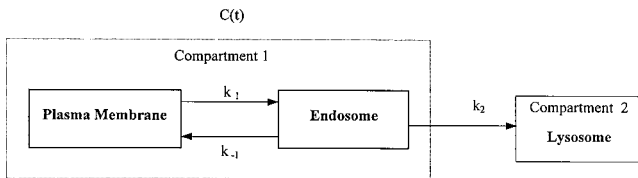
Because the only available information for evaluating half-life is the recycling time and the efficiency, λ, which refers to the proportion of amount not degraded after each round of recycling, the two compartments are viewed as one compartment denoted by $C(t)$. The following differential equation describes the above-mentioned system:

$$\frac{d}{dt} C(t) = -k_2 C(t) \tag{1}$$

where k_2 is a positive real number. Solving the above-mentioned differential equation, we have,

$$C(t) = C_0 \exp(-k_2 t), \text{ such that } C(0) = C_0 \tag{2}$$

Note that t can be written as $t = r + np$, where n denotes the number of times a molecule is recycled, p refers to amount of time required for one cycle, and r is the remainder of time after the last cycle. Let $t_1 = r_1 + np$ and $t_2 = r_1 = (n + 1)p$, then efficiency, λ, can be written as,

$$\lambda = \frac{C(t_1)}{C(t_2)} = \frac{C_0 \exp(-k_2 t_1)}{C_0 \exp(-k_2 t_2)} = \exp[-k_2(t_2 - t_1)] \tag{3}$$
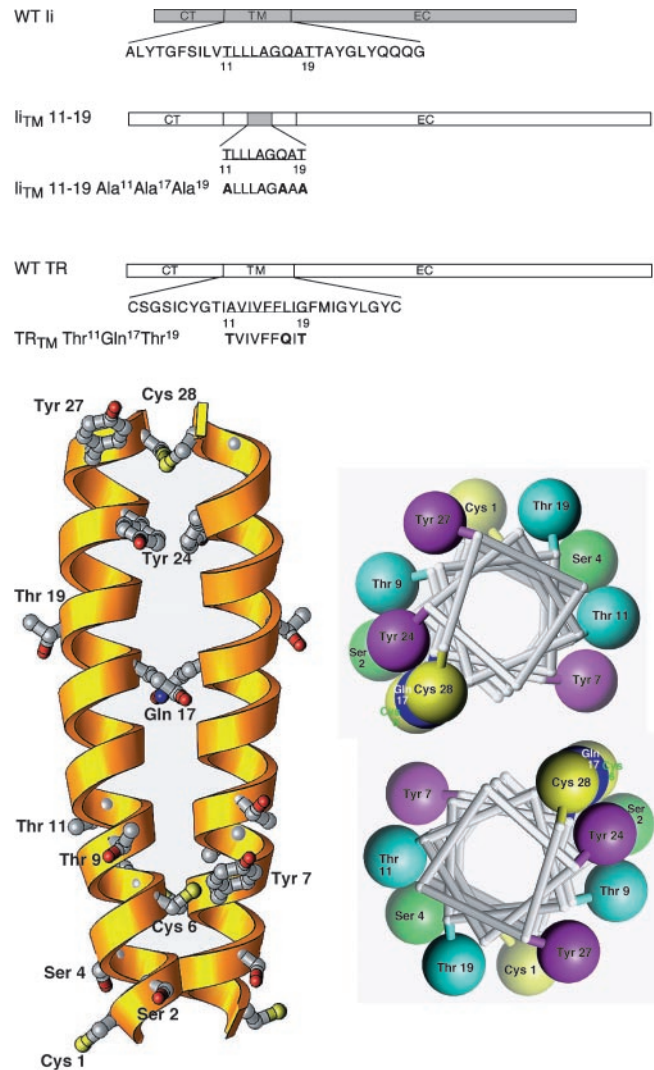
$$= \exp[-k_2(r_1 + (n + 1)p - r_1 - np)] \tag{4}$$

$$= \exp[-k_2 p] \tag{5}$$

It follows that,

$$k_2 = -\ln(\lambda)/p \tag{6}$$

Substituting k_2 in Eq. 2, the compartment size is simplified to,

$$C(t) = C_0 \exp\left[\frac{\ln(\lambda)}{p} t\right] \tag{7}$$

Figure 1. (A) Schematic diagram of the TR$_{TM}$ mutants. A schematic diagram is shown of the MHC class II Ii showing the wild-type TM sequence. The Ii$_{TM}$ 11–19 chimera contains a nine-amino acid substitution (shaded area) from the Ii that promotes lysosomal targeting (Kang *et al.*, 1998). All other portions of this chimera are derived from the wild-type TR (unshaded areas). For each of the TM mutants prepared, the amino acid substitutions are shown. Constructs are referred to throughout by the corresponding names shown on the left. (B) Structural models for the TR dimeric TM. Left, three-dimensional ribbon model of the TM of the TR$_{TM}$ Thr^{11}Gln^{17}Thr^{19} mutant, represented as a helical dimer with the carboxy-terminus at the top. Only side chains of polar residues are depicted. The numbering system shown is the same as that used in Figure 1. Right, helical wheel representation of the same dimer, viewed from the carboxy-terminal end of the helix. Only polar residues are depicted. The software program Ribbons 3.1 was used (Carson, 1997).

Thus, the half-life of a protein at the cell surface becomes

$$t_{1/2} = \frac{p\ln(0.5)}{\ln(\lambda)} \tag{8}$$
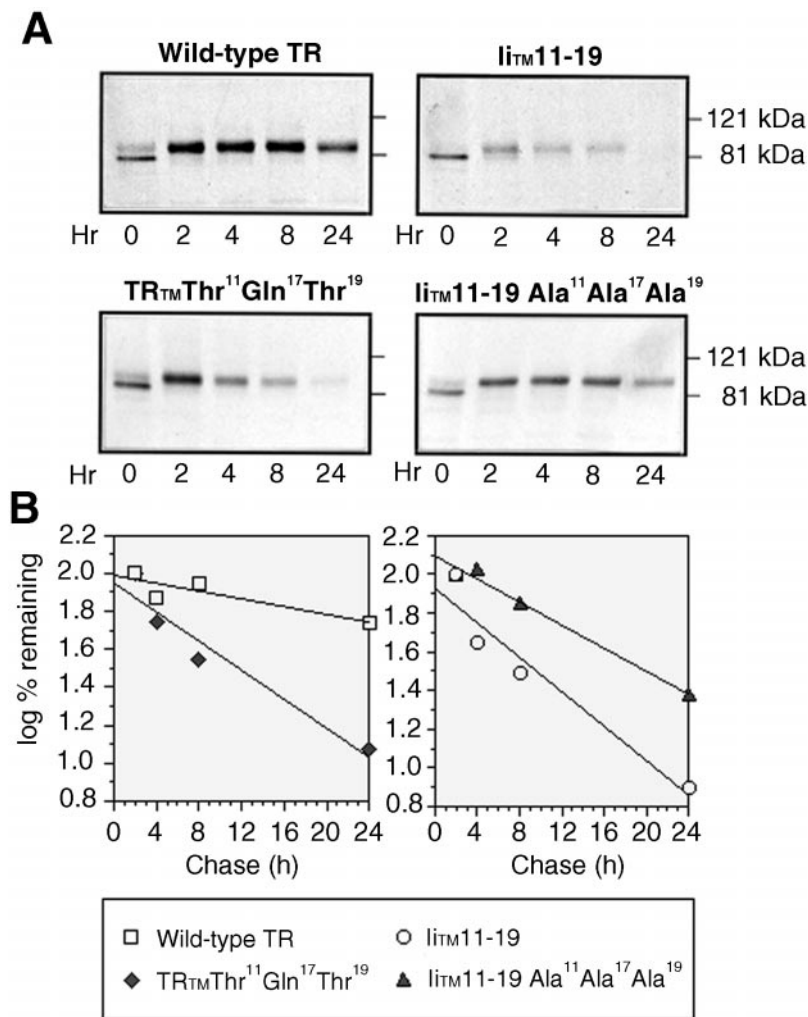
Figure 2. Polar residues in the TR TM are necessary and sufficient to mediate targeting of the TR to a post-Golgi–processing compartment. Equivalent cell numbers of CEFs expressing wild-type TR, Ii_{TM} 11–19, TR_{TM} $Thr^{11}Gln^{17}Thr^{19}$, and Ii_{TM} 11–19 $Ala^{11}Ala^{17}Ala^{19}$ chimeras were pulse labeled for 30 min with *trans*-^{35}S label and chased with complete medium for various periods of time as indicated. Wild-type or mutant TRs were then immunoprecipitated from postnuclear supernatants and analyzed on SDS-polyacrylamide gels (A) as described under MATERIALS AND METHODS. Dried gels were exposed to XAR film overnight (Kodak). Radioactivity in the bands was quantitated on a PhorphorImager (B). A representative experiment of four is shown.

Because the transit time for a newly synthesized membrane protein to reach the cell surface (t_{sur}) must be taken into account for the half-life calculation, the half-life becomes,

$$t_{1/2} = \frac{p\ln(0.5)}{\ln(\lambda)} + t_{sur} \tag{9}$$

With this equation, a cell surface molecule half-life ($t_{1/2}$) can be estimated from recycling efficiency (λ), the period of time required for one cycle (p), and the time required for a newly synthesized membrane protein to reach the cell surface from the biosynthetic pathway (t_{sur}). For example, if the membrane protein requires 1 h for transit to the cell surface, its recycling efficiency is 98%, and the period of time required for one cycle is 40 min (i.e., 0.6667 h), then the estimated half-life of the protein ($t_{1/2}$) = 0.6667 ln (0.5)/ln 0.98 + 1 h is,

$$t_{1/2} = [0.6667\ln(0.5)/\ln(0.98)] + 1 \text{ h} \tag{10}$$

$$= [0.6667(-0.6931)/(-0.0202)] + 1 \text{ h} \tag{11}$$

$$= 23.9 \text{ h} \tag{12}$$

Analytical Ultracentrifugation

Sedimentation equilibrium experiments were conducted on Beckman XL-A Analytical ultracentrifuge equipped with absorption optics with a four-cell An-60 Ti rotor with Beckman Optima XL-A/XL-I data analysis software (version 4.0). Peptides were dissolved in 80% trifluroethanol in H_2O to a final concentration of 2 mg/ml. Synthetic boundary cells were loaded with 120 μl of solute with the reference sector filled with 130 μl of 80% trifluroethanol in H_2O. Samples were centrifuged at 60,000 rpm for 30 h to allow the system to reach equilibrium. Scans were taken at the wavelength 265 nm at radial increments of 0.001 cm. Equilibrium distributions were fitted for the molar mass of the solute by standard numerical analysis with the program Microcal Origin 4.1 (MicroCal Software, Northampton, MA; www.microcal. com). The partial specific volumes of peptides were calculated from their amino acid composition: wild-type TR_{TM} 11–19 (0.81 ml/g) and Ii_{TM} 11–19 (0.76 ml/g). The density of the solvent was determined to be 1.32645 g/ml with SEDNTRP program (Hansen *et al.*, 1994, no. 2740).

RESULTS

Polar Residues in the TM Promote Degradation in a Post-Golgi-processing Compartment

Previous studies demonstrated that a TR chimera containing a nine-residue substitution in the middle portion of the TM from the MHC class II Ii (Kang *et al.*, 1998) was efficiently delivered to the lysosomal compartment. Because this re-
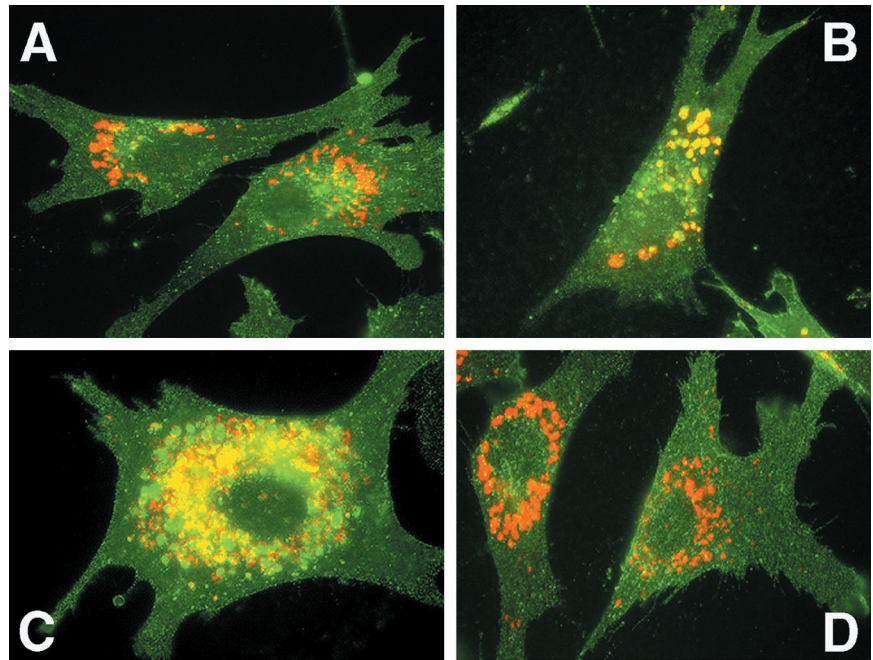
Figure 3. Colocalization of wild-type and mutant TR with LEP100. CEF expressing wild-type TR (A), TR_{TM} $Thr^{11}Gln^{17}Thr^{19}$ (B), Ii_{TM} 11–19 (C), and Ii_{TM} 11–19 $Ala^{11}Ala^{17}Ala^{19}$ (D) were fixed, permeabilized, and stained with rabbit anti-TR antisera followed by Oregon Green-labeled goat anti-rabbit Ig or mouse anti-LEP100 followed by Texas Red-labeled goat anti-mouse IgG. Colocalization of the two proteins is indicated by yellow fluorescence.

gion of the Ii contains a number of noncharged polar residues, including one Gln and two Thr residues (whereas the wild-type TR did not), we hypothesized that these amino acids might influence lysosomal targeting. To test this, we constructed two mutants. In the first, we removed all of the polar residues from the Ii_{TM} 11–19 by replacing them with alanines (Ii_{TM} 11–19 $Ala^{11}Ala^{17}Ala^{19}$; Figure 1A). In the second, we replaced three residues in the wild-type TR with the polar residues, inserting them in the same positions as found in the Ii_{TM} 11–19 mutant (TR_{TM} $Thr^{11}Gln^{17}Thr^{19}$; Figure 1B). Although the structure of the TM domain is not known, it is established that the TR is a dimer with a disulfide bridge at residue 89 (right at the TM/extracellular domain interface; Jing and Trowbridge, 1987). Assuming that the TR traverses the lipid bilayer as a helix and that the alignment of the helices is dictated by the disulfide bond at residue 89 (residue 28 in the TM), this places the Thr residues on the outside and the Gln on the inside at the dimer interface (Figure 1B). This orientation also places the major acylation site, Cys 62 (Jing and Trowbridge, 1987), with the acyl chains pointing out into the bilayer, lending credence to the proposed model. Using these introduced modifications, we tested the hypothesis that the polar residues influenced the trafficking of the TR.
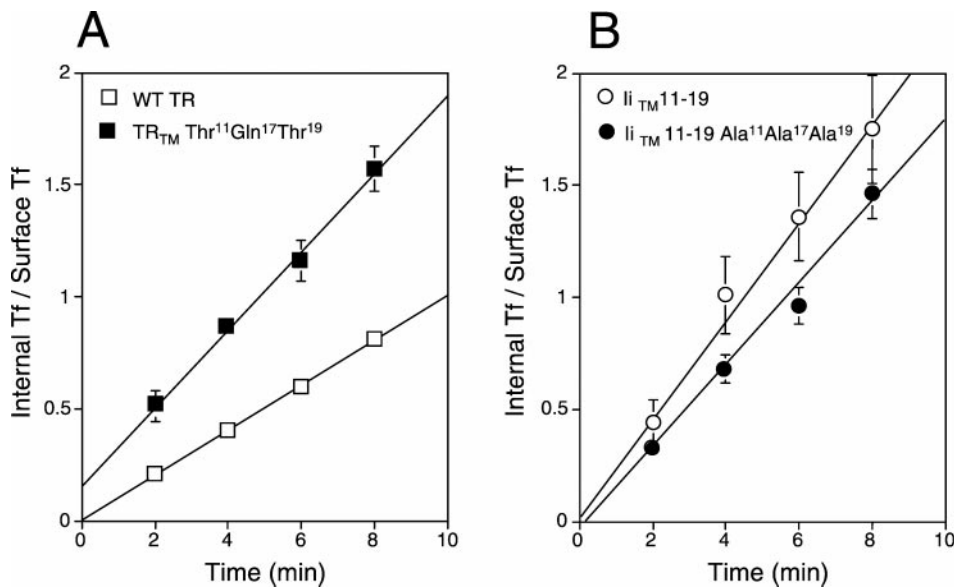
Ii_{TM} 11–19, Ii_{TM} 11–19 $Ala^{11}Ala^{17}Ala^{19}$, wild-type TR, and TR_{TM} $Thr^{11}Gln^{17}Thr^{19}$ were stably expressed in CEFs with BH-RCAS, a replication-competent retroviral vector derived from the Rous-sarcoma virus (Hughes *et al.*, 1990). Binding studies at 4°C with ^{125}I-labeled Tf indicated that all of the chimeras/mutants were expressed on the cell surface and that each, like the wild-type TR, was a ~200-kDa dimer on a nonreducing SDS-PAGE gel (our unpublished results).

To determine the effects of the mutations on the half-lives of the constructs, we performed metabolic pulse–chase experiments. CEFs expressing either wild-type TR, Ii_{TM} 11–19, TR_{TM} $Thr^{11}Gln^{17}Thr^{19}$, or the Ii_{TM} 11–19 $Ala^{11}Ala^{17}Ala^{19}$

mutant were pulse-labeled with *trans*-^{35}S label for 30 min and chased in complete media for the indicated periods of time; TR and TR mutants were then isolated by immunoprecipitation and analyzed by SDS-PAGE (Figure 2). The wild-type TR and the Ii_{TM} 11–19 mutant had half-lives of 26.9 ± 4.6 h (mean ± SE) and 5.4 ± 0.8 h, respectively. Interestingly, the TR_{TM} $Thr^{11}Gln^{17}Thr^{19}$ mutant had a greatly reduced half-life (5.6 ± 0.7 h), whereas the Ii_{TM} $Ala^{11}Ala^{17}Ala^{19}$ mutant had an extended half-life (14.8 ± 1.9 h). After 2 h (Figure 2), the M_r of TR and each of the mutants increased to that of the mature glycoprotein (Omary and Trowbridge, 1981), indicating that all of the mutants traverse the Golgi where glycosylation is complete. Because the maturely glycosylated form of each of the mutants was disappearing, this suggested that the degradation occurred in a post-Golgi compartment.

Degradation Occurs in the Lysosomal Compartment

To confirm that the rapid degradation was due to delivery to the lysosomal compartment, we compared the intracellular distributions of each of the TR mutants with LEP100, an endogenous chicken lysosomal membrane protein (Lippincott-Schwartz and Fambrough, 1986, 1987). The wild-type TR shows a typical punctate staining (shown in green, Figure 3A) with very little overlap with LEP100 (shown in red). The TR_{TM} $Thr^{11}Gln^{17}Thr^{19}$ mutant, however, shows an altered intracellular distribution with significant overlap with LEP100 (Figure 3B). The Ii_{TM} 11–19 mutant shows a similar colocalization with LEP100 (Figure 3C). Interestingly, the mutant with the polar residues removed, Ii_{TM} $Ala^{11}Ala^{17}Ala^{19}$, has a distribution pattern very similar to the wild-type TR (Figure 3D), indicating that the TR_{TM} $Thr^{11}Gln^{17}Thr^{19}$ and Ii_{TM} 11–19 mutants traffic along the prelysosomal segment of the endocytic pathway. These re-

A

B

Figure 4. Comparison of internalization rates of wild-type TR and various TR TM mutants. Equivalent numbers of CEFs expressing wild-type TR and TR_{TM} $Thr^{11}Gln^{17}Thr^{19}$ (A) or Ii_{TM} 11–19 and Ii_{TM} 11–19 $Ala^{11}Ala^{17}Ala^{19}$ chimeras (B) were incubated with prewarmed (37°C) ^{125}I-labeled Tf for indicated times. The amounts of internalized (internal Tf) and surface associated (surface Tf) radiolabel were determined as described under MATERIALS AND METHODS. Data are plotted with IN/SUR method, in which the slope of the line equals the endocytic rate constant k_e (Wiley and Cunningham, 1982). The data represent the mean ± SE from five experiments for each time point.

sults indicate that polar residues within the TM are both necessary and sufficient for lysosomal targeting.

Internalization Is Affected by Amino Acid Substitutions in the TM

Because the substitutions dramatically affected the half-life and intracellular distributions of the proteins, we next tested whether these modifications affected endocytosis. The internalization rates of the chimeras were monitored with the IN/SUR method of Wiley and Cunningham (1982). Surprisingly, analysis of the TR_{TM} $Thr^{11}Gln^{17}Thr^{19}$ mutant indicated that it was internalized 79% faster than the wild-type TR ($k_e = 0.200 \pm 0.046$ min^{-1} versus 0.112 ± 0.015 min^{-1}), making it comparable to the Ii_{TM} 11–19 mutant ($k_e = 0.245 \pm 0.089$ min^{-1}). Analysis of the Ii_{TM} 11–19 $Ala^{11}Ala^{17}Ala^{19}$ mutant indicated that it was internalized 26% slower than the Ii_{TM} 11–19 mutant ($k_e = 0.180 \pm 0.055$ min^{-1}), but still significantly faster than the wild-type TR (Figure 4). This indicated all of the constructs that contained polar residues within the TM were internalized significantly faster than the wild-type TR.

Polar Residues in the TM Inhibit Receptor Recycling

Because delivery of the proteins to the lysosomal compartment could be mediated by sorting from the trans-Golgi network or the cell surface (Kang *et al.*, 1998), we tested the effects of the TM mutations on receptor recycling. Cells expressing TR, TR_{TM} $Thr^{11}Gln^{17}Thr^{19}$, Ii_{TM} 11–19, or Ii_{TM} 11–19 $Ala^{11}Ala^{17}Ala^{19}$ were incubated with ^{125}I-labeled Tf for 10 min at 37°C. The cells were then rapidly rinsed with PBS to remove any unbound label and prewarmed media (37°C) was then added to the cells. The reappearance of intact and degraded Tf in the medium was monitored by measuring TCA insoluble and soluble radioactivity, respectively. As expected, the apo-Tf that was released into the medium from cells expressing the wild-type TR was undegraded because only $2.9 \pm 0.1\%$ of the radioactivity was in

the TCA soluble pool (Figure 5). This suggested that >97% of the receptors were recycled back to the cell surface. In contrast, $7.1 \pm 0.1\%$ of the ^{125}I-labeled Tf released from cells expressing the TR_{TM} $Thr^{11}Gln^{17}Thr^{19}$ mutant were degraded, implying that this percentage of the mutant receptors traffic directly from the cell surface to the lysosomal compartment where they are degraded. Interestingly, a similar amount of ^{125}I-labeled Tf was released as TCA soluble counts from cells expressing the Ii_{TM} 11–19 mutant, $7.8 \pm 0.4\%$, suggesting that the polar residues within this TM sequence were sufficient to inhibit efficient recycling. Further support for this is shown with the Ii_{TM} $Ala^{11}Ala^{17}Ala^{19}$ mutant, which appears to be recycled at nearly wild-type levels (4.1 ± 0.1% TCA soluble counts), suggesting that the polar residues in the Ii_{TM} 11–19 mutant were responsible for the loss of efficient recycling. Furthermore, the amount of cell-associated radioactivity of the Ii_{TM} 11–19 and TR_{TM} $Thr^{11}Gln^{17}Thr^{19}$ mutants (base counts) was much higher than the wild-type TR or Ii_{TM} 11–19 $Ala^{11}Ala^{17}Ala^{19}$ (19.8 ± 1.2 and $14.2 \pm 1.5\%$ versus 4.7 ± 0.1 and $8.7 \pm 0.7\%$, respectively), providing additional evidence that these mutants were not as efficiently recycled as the wild-type TR.

Polar Residues in the TM Promote Self-Association of TRs

To monitor differences in the association properties of the TRs, we analyzed the wild-type TR and TR mutants in sucrose gradients. Cell lysates from metabolically labeled CEFs expressing TR and TR mutants were loaded onto 10–25% sucrose gradients and centrifuged at 40,000 rpm in a SW 50.1 rotor for 16 h at 4°C. Fractions were collected and TR, TR_{TM} $Thr^{11}Gln^{17}Thr^{19}$, Ii_{TM} 11–19, or Ii_{TM} 11–19 $Ala^{11}Ala^{17}Ala^{19}$ were immunoprecipitated and analyzed by SDS-PAGE and autoradiography (Figure 6). The results indicated that the wild-type TR and Ii_{TM} $Ala^{11}Ala^{17}Ala^{19}$ sedimented with an S value of 6.9 and 7.4, respectively, whereas the Ii_{TM} 11–19 sedimented with an
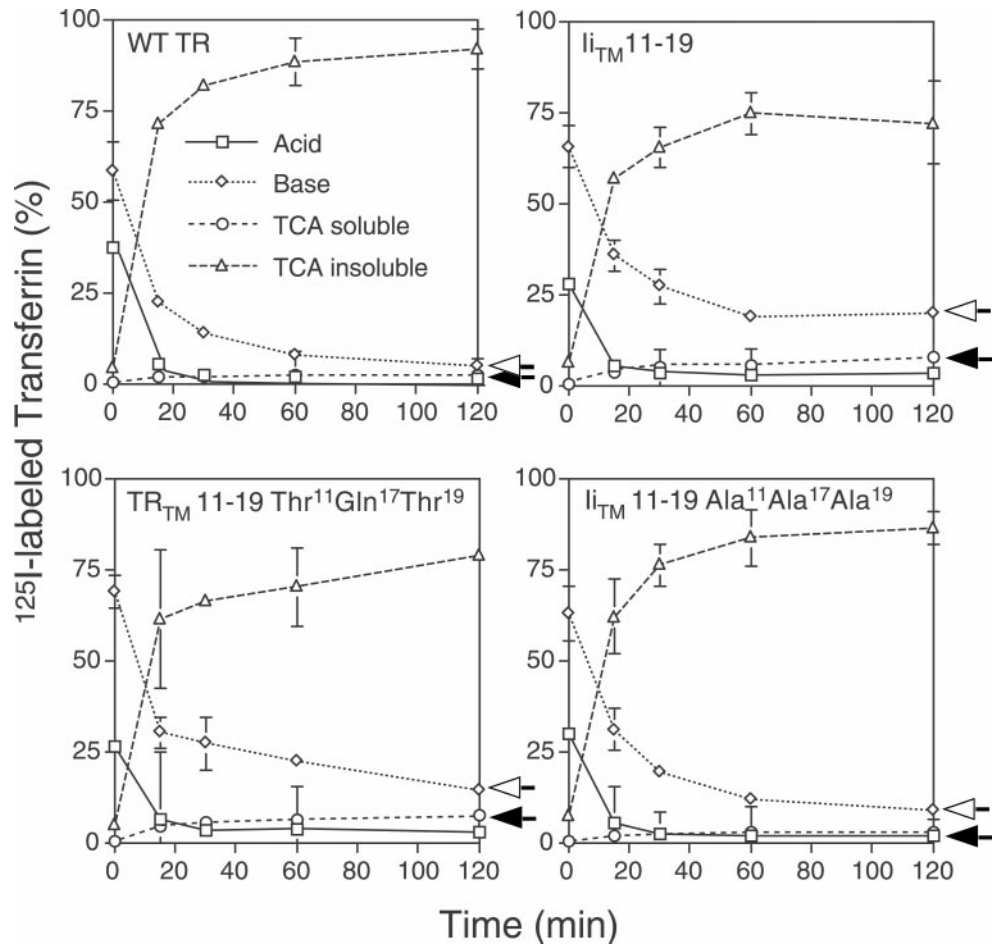
Figure 5. Degradation of Tf bound to wild-type TR and TR TM mutants. Equivalent cell numbers of CEFs expressing wild-type TR, Ii_{TM} 11–19, TR_{TM} $Thr^{11}Gln^{17}Thr^{19}$, and Ii_{TM} 11–19 $Ala^{11}Ala^{17}Ala^{19}$ were preincubated in serum-free medium for 30 min at 37°C and then incubated with ^{125}I-labeled Tf in BSA-PBS for 10 min. at 37°C. The cells were then washed and reincubated at 37°C in DMEM containing 50 μg/ml unlabeled Tf and 0.1% BSA for various times. Acid-soluble radioactivity (○) or acid-insoluble ^{125}I-labeled Tf (△) released into the medium, as well as surface bound Tf (acid, □) and internalized (base, ◇) ^{125}I-labeled Tf was determined as described under MATERIALS AND METHODS and is expressed as a percentage of total radioactivity recovered. Each data point is the mean ± SE from an experiment done in triplicate. A representative experiment of three is shown.

S value of 9.5. The TR_{TM} $Thr^{11}Gln^{17}Thr^{19}$ mutant was more diffuse in the gradient and sedimented in what appeared to be two populations with S values of 7.8 and 9.1. The second population appeared as a shoulder with 11% of the protein in this fraction, compared with the wild-type TR, which contained 5% protein in this same fraction. These results are consistent with the wild-type and Ii_{TM} $Ala^{11}Ala^{17}Ala^{19}$ being dimers, the Ii_{TM} 11–19 being a tetramer, and the TR_{TM} $Thr^{11}Gln^{17}Thr^{19}$ being a combination of dimers and tetramers (Alvarez *et al.*, 1989). This analysis indicated that the presence of polar residues in the TR TMs promoted tetramer and perhaps larger aggregate formation, supporting the view that the polar residues affected the self-association properties of the complexes.

To confirm this result with another method, we analyzed the TR mutants by the use of chemical cross-linking. Cells expressing either wild-type TR or a TR mutant were metabolically labeled and chased in complete medium for 2 h to ensure that all of the labeled TRs were maturely glycosylated. Cells were then lysed and the postnuclear supernatants were incubated at room temperature with 1 mM DTSSP for 20 min and the reaction stopped with 50 mM Tris in lysis buffer. Cross-linked samples were immunoprecipitated and analyzed by SDS-PAGE to eval-

uate the extent of cross-linking (Figure 7). The results indicate for the wild-type TR the majority of the complexes formed by cross-linking were dimers (72% of the label as measured by PhosphorImage analysis), with very little protein running as larger complexes. Analysis of the TR_{TM} $Thr^{11}Gln^{17}Thr^{19}$ and Ii_{TM} 11–19 mutants, however, indicated that the amount of dimer decreased to 25 and 18%, respectively, whereas the Ii_{TM} 11–19 $Ala^{11}Ala^{17}Ala^{19}$ mutant had 52% dimer, suggesting a partial recovery. Although the absolute amounts of the different forms of cross-linked material are difficult to quantitate from this type of an experiment, the results clearly indicate that there is a difference in the amount of dimer found for each of the constructs. The nondimeric forms of the proteins ran as higher MW complexes with some material running at the top of the stacking gel. Together, the sucrose gradient and cross-linking studies indicate that the association properties of the TR mutants were affected by the addition of the polar residues.

Cross-linked Tf Complexes Promote Lysosomal Targeting of Wild-Type TR

If polar residues in the TM region promote lysosomal targeting through self-association of receptors, then other
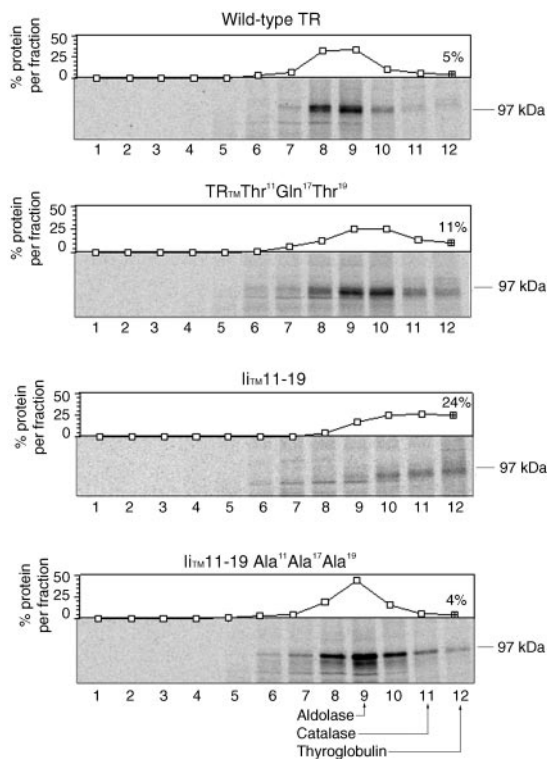
Figure 6. Sucrose gradient sedimentation of TR TM mutants. CEF cells expressing wild-type TR, TR$_{TM}$ Thr^{11}Gln^{17}Thr^{19}, Ii$_{TM}$ 11–19, and Ii$_{TM}$ 11–19 Ala^{11}Ala^{17}Ala^{19} were pulse labeled with *trans*-^{35}S label for 2 h and chased 1 h in complete medium. Lysates were loaded onto 5–25% sucrose gradients and centrifuged as described under MATERIALS AND METHODS. Fractions were collected (numbering is from the top of the gradient), immunoprecipitated with anti-TR antibody, and analyzed by SDS-PAGE. Dried gels were exposed to XAR film (Kodak) overnight. Immunoprecipitates were quantitated on a PhosphorImager and the relative amounts in each fraction are shown above. The positions of molecular weight standards are shown: A, aldolase (7.4S); B, catalase (11.3S); and C, thyroglobulin (19.3S). A representative experiment of three is shown.

mechanisms leading to native receptor self-association should have the same effect. To test this idea, we prepared cross-linked Tf with glutaraldehyde. The cross-linked material was purified by gel filtration and separated into MW complexes >160 kDa (fraction 1) and ~160 kDa (fraction 2; our unpublished results). Cross-linked (fraction 2) and native Tf were then ^{125}I-labeled. Cells expressing the wild-type TR were incubated with ^{125}I-labeled monomeric and cross-linked Tf for 10 min at 37°C. The cells were then rapidly washed, and the reappearance of intact and degraded Tf in the medium was monitored by measuring TCA insoluble and soluble radioactivity as described above. As expected, the Tf released from cells incubated with the monomeric Tf was mostly TCA insoluble, with only 2.6 ± 0.1% in the TCA-soluble pool (Figure 8A), whereas 18.7 ± 1.7% was in the TCA-soluble pool from cells incubated with the cross-linked Tf (Figure 8B), suggesting that recycling had been dramatically inhibited. Because this fraction contained dimeric Tf (~160 kDa of material; Tf monomer is 80 kDa), this suggested that cross-linking the receptors resulted in down-regulation of the complexes, supporting the view that cross-linking receptors, by any mechanism, results in a loss of recycling efficiency.

DISCUSSION

The TR is the prototype for a recycling receptor and during its lifetime recycles 100 times or more. Although a number of studies, including our own, have examined the structural features within the cytoplasmic tails of proteins that are important for internalization and/or lysosomal targeting, very little information is available regarding the role of the TM residues in these processes. In this study, we have carefully analyzed the effect of mutations within the TM on the fidelity of recycling and found that the insertion of Thr and Gln residues inhibits receptor recycling, thereby promoting down-regulation. Furthermore, we demonstrated that small changes in the recycling efficiency dramatically alter the half-life of the receptors, providing an alternative mechanism for down-regulation of cell surface receptors that bypasses the need for a specific cytoplas-
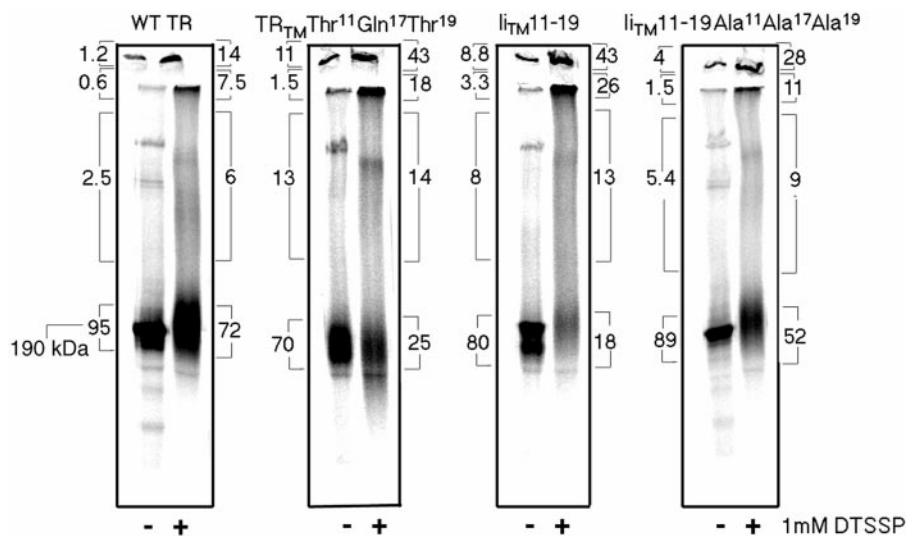
Figure 7. Analysis of TR TM mutants by chemical cross-linking. CEF cells expressing wild-type TR, TR$_{TM}$ Thr^{11}Gln^{17}Thr^{19}, Ii$_{TM}$ 11–19, and Ii$_{TM}$ 11–19 Ala^{11}Ala^{17}Ala^{19} were pulse labeled with *trans*-^{35}S label overnight and chased in complete medium for 2 h. Cells were lysed in 1% Triton X-100 and the cell lysates were cross-linked with 1 mM DTSSP for 20 min at room temperature. Receptors were isolated by immunoprecipitation, analyzed by SDS-PAGE under nonreducing conditions, and quantitated on a Phosphoimager. Bracketed numbers indicate the percentage of total protein present in each fraction. A representative experiment of three is shown.

Figure 8. Degradation of Tf and cross-linked Tf bound to the wild-type TR. CEFs expressing wild-type TR were preincubated in serum-free medium for 30 min at 37°C and then incubated with ^{125}I-labeled Tf or ^{125}I-labeled cross-linked Tf for 10 min. at 37°C. The cells were then washed and reincubated at 37°C in DMEM containing 50 μg/ml unlabeled Tf and 0.1% BSA for various times. Acid-soluble radioactivity ($\bigcirc$) or acid-insoluble ^{125}I-labeled Tf ($\triangle$) released into the medium, as well as surface bound Tf ($\square$) and internalized ($\diamond$) ^{125}I-labeled Tf was determined as described in Figure 5. A representative experiment of three is shown.
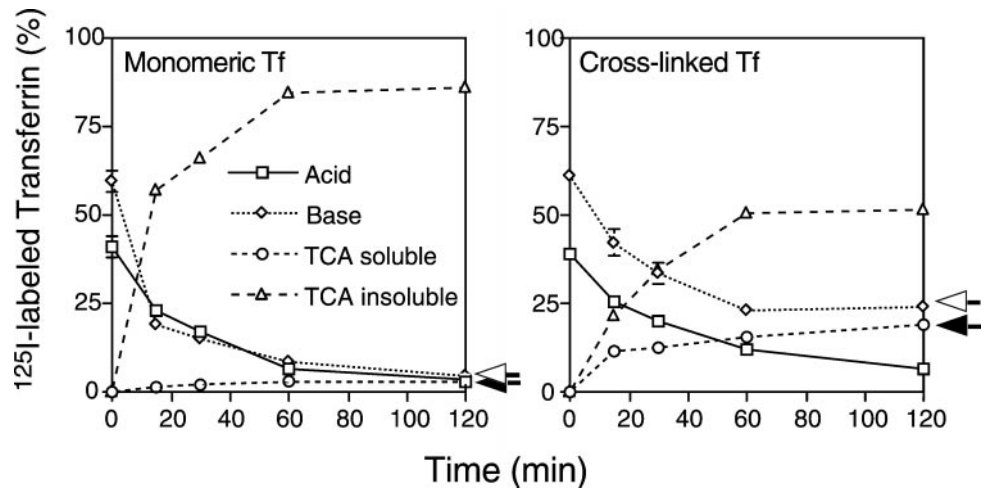
mic tail sorting signal. By developing a mathematical model for recycling efficiency, we demonstrated that a loss of as little as ~8% recycling efficiency dramatically alters the half-lives of proteins trafficking in this pathway. For growth factor receptors, this would represent an effective mechanism for receptor clearance.

Because Golgi protein localization studies suggest that TM polar residues promote self-association (Weisz *et al.*, 1993), we tested whether this same phenomenon was true in our TR mutants. Results from both sucrose gradient analysis and the chemical cross-linker studies supported the view that receptor self-association correlated with down-regulation. Further support for this idea came from cross-linking the wild-type receptor with dimeric Tf, which also resulted in effective down-regulation of the complexes. This last result is consistent with previous studies that showed that the TR was rapidly degraded after monoclonal antibody cross-linking (Weissman *et al.*, 1986).

Our results are consistent with those of Maxfield and coworkers (Marsh *et al.*, 1995) who demonstrated that oligomerized TRs were retained in the recycling compartment in TRVb-1 cells. In spite of the fact that Maxfield and coworkers were following the trafficking of a cross-linked Tf complex composed of an average of 10 Tf molecules rather than the dimeric Tf molecules we were using, both studies support the view that cross-linked Tf recycles more slowly. In our studies, ~25% of the cross-linked Tf was still intracellular after 2 h of chase. In our study, however, it remains unclear how much of that intracellular material was in the lysosome versus the recycling compartment. Interestingly, Marsh *et al.* (1995) did see an increase in the amount of TCA-soluble counts released into the media, albeit to a lesser degree than we did.

One of the obvious questions resulting from our study is how do polar residues mediate this effect? There seem to be a number of possibilities that could explain our results. First, the polar residues within the TM promoted self-association directly. When we analyzed the sedimentation properties of peptides derived from the TM region in nonpolar solvents (see MATERIALS AND METHODS), we found that those peptides containing the Thr and Gln residues aggregated (the average MW calculated from sedimentation equilibrium

measurements was 5409, range 4569 to 6242), whereas peptides derived from the wild-type TR sequence sedimented as a monomer (MW ~466, range 442 to 490; our unpublished results), lending support for this hypothesis. A second possibility is that the self-association properties could be mediated through the extracellular domains. Recent studies with cryo-electron microscopy on the TR reconstituted in phospholipid vesicles indicate that the TR dimer consists of a large globular extracellular domain (6.4 × 7.5 × 10.5 nm) separated from the membrane by a thin molecular stalk (2.9 nm; Fuchs *et al.*, 1998). Because the large extracellular domains of the dimer are tethered together through these closely associated stalks that traverse the membrane, it is conceivable that self-association occurs through the extracellular domains. Because the TR undergoes a conformation change at the pH found in the sorting endosome (Turkewitz *et al.*, 1988), it is possible that these substitutions affect the conformational changes in the sorting endosome. Furthermore, alterations in the TR conformational changes may in turn affect the self-associating properties of the complexes. A third possibility that we cannot rule out is that the TM modifications affect the conformation of the TR cytoplasmic tail. This idea is certainly consistent with the fact that these mutations dramatically alter the TR internalization rate. An

Table 1. Comparison of the amino acid sequences of the human, mouse, hamster, and chicken TR TM

Species	Amino acid sequence
	11 17 19
Human[a]	CSGSIC**YGTIA**VIVFF**LIGF**MI**GYL**GYC
Mouse[b]	LCFAA**IA**LVIFF**LIGF**MS**GYL**GYC
Hamster[c]	LCFGT**IA**VVIFF**LIGF**MI**GYL**GLC
Chicken[d]	LCFLV**IA**AVLLL**LIGF**LI**GYL**SY

[a] McClelland *et al.* (1984).

[b] Trowbridge *et al.* (1988).

[c] Collawn *et al.* (1993).

[d] Gerhardt *et al.* (1991).

Table 2. Membrane proteins targeted to the prelysosomal/lysosomal compartment containing uncharged, polar residues in the TM

Protein	Name and function	Destination	TM sequences	Reference
L-MAG (human)	Myelin-associated glycoprotein Adhesion molecule required for maintaining myelin-forming cell-axon contact	Endocytosed and lysosomally degraded in quaking mice	VGAVVAFAILIAIC**Y**I**TQT**	(Bo *et al.*, 1995)
CD19 (mouse)	CD19 Part of the signal transduction complex in B lymphocytes	Internalized and down-regulated; cytoplasmic tail is not required for internalization	**W**IVPVV**T**LV**Y**VIFCMV**S**LVAFL**Y**C	(Bradbury *et al.*, 1993)
CD40L (human, mouse)	CD40L T cell activation molecule associated with T-BAM	Internalized and down-regulated after interaction with CD40 molecules on B cells	IFM**Y**LL**T**VFLI**TQ**MIF**S**ALFAV**Y**L	(Yellin *et al.*, 1994)
CD3-δ-γ (human)	CD3 Part of the T cell receptor-signaling complex	Internalized and degraded in the lysosome	PA**T**VAFIIV**T**DVIA**T**LLLALGVFCFAG	(Letourneur and Klausner, 1992)
Interleukin-1 receptor (human)	Interleukin-1 receptor Proliferation of helper T cells (Th2)	Internalized and degraded in the lysosome	HVIGICV**T**L**T**VIIVC**S**VFI**Y**	(Solari *et al.*, 1994)
Ii (human)	MHC class II Ii Targets the MHC class II-α-β chains to the lysosomal compartment	Internalized and delivered to the lysosomal compartment	GAL**YT**GF**S**ILV**T**LLLAG**Q**A**TTA Y**FL**Y**	(Bakke and Dobberstein, 1990)
Fc receptor (mouse)	Macrophage Fc receptor Clearance of IgG-containing immune complexes	Internalized and delivered to lysosomal compartment after binding polyvalent immune complexes	VL**T**IVAAV**T**GIAVAAIVIILV**S**LV**Y**L	(Mellman and Plutner, 1984)
Mannose 6-phosphate receptor (human)	Cation-independent mannose 6-phosphate receptor (IGF receptor) Uptake of lysosomal enzymes	Internalized and is delivered to late endosome; escapes lysosomal targeting because it contains a TGN-sorting signal	AVGAVL**S**LLLVAL**T**CCLLALLL**Y**	(Oka *et al.*, 1985; Diaz and Pfeffer, 1998)
Fibroblast growth factor receptor (human)	Fibroblast growth factor receptor	Internalized and delivered to lysosomal compartment after ligand binding	III**Y**C**T**GAFLI**S**CMVG**S**VIV**Y**	(Sorokin *et al.*, 1994)
Mannose receptor (human)	Macrophage mannose receptor lectin that binds and internalizes proteins containing terminal mannose residues	Internalized; important for delivery of antigens to the antigen-processing compartment	P**SS**NVAGVVIIVILLIL**T**GAGLAA**Y**FF**Y**	(Wileman *et al.*, 1986; Jiang *et al.*, 1995)
Chicken hepatic lectin receptor (chicken)	Chicken liver glycoprotein receptor Lectin	Internalizes and recycles several times before being delivered to the lysosomal compartment	**S**FAAV**Y**VLLAL**S**FLLL**T**LL**SS**V**S**LA	(Mellow *et al.*, 1988; Graeve *et al.*, 1989)
P-selectin (mouse)	Adhesion molecule on activated platelets as a receptor for leukocytes	Internalized and targeted to lysosomes	L**TY**LGGAVA**STT**GLEVGG**T**LLALL	(Green *et al.*, 1994)

altered cytoplasmic tail conformation might allow for a better interaction with the adaptor complexes in the coated pits. An even simpler explanation would be that enhanced self-association of the receptors would bring a higher concentration of complexes into the pit, translating into a more efficient internalization rate. A fourth possibility is that the inclusion of polar residues promotes association of the TRs with other proteins in the sorting endosome that are being

down-regulated. Although we do not believe this is the case because we have never detected other protein bands either with chemical cross-linking or from TR immunoprecipitations, we cannot rule out this possibility.

How might self-association of receptor complexes in the sorting endosome result in down-regulation and lysosomal targeting? Recent studies on lipid trafficking in the endocytic pathway suggest that lipid sorting depends on the chemistry

Table 3. Comparison of the experimental and calculated recycling efficiencies of TR mutants

Protein	Recycling efficiency (%)	Experimental half-life (h)	Calculated half-life (h)
Wild-type TR	98[a]	27 ± 4.6[b] (6)[c]	23.9
TR_{TM} Thr[11]Gln[17]Thr[19]	93	5.4 ± 0.8 (7)	7.4
Ii_{TM} 11–19	92	5.6 ± 0.7 (7)	6.5
Ii_{TM} 11–19 Ala[11]Ala[17]Ala[19]	96	15 ± 1.9 (7)	12.3

[a] Based on 2% TCA-soluble counts in the media after 2 h. See MATERIALS AND METHODS for details of the calculation.
[b] Mean ± SE.
[c] Number of independent experiments.

of the lipid hydrophobic tails (Mukherjee *et al.*, 1999). This intriguing study demonstrated that lipids with long (16-carbon) saturated tails are delivered to late endosomes, whereas lipids with two *cis* double bonds or with saturated but shorter tails (12-carbon) are delivered to the recycling compartment. In their model, Mukherjee *et al.* (1999) propose that lipid trafficking in the endocytic and other pathways depends on differences in fluidity. They suggest that those lipids with long unsaturated tails preferentially partition into domains that are more ordered and unsaturated or shorter tails partition into more fluid regions of the bilayer.

In support of this model, recent studies have shown that long saturated glycosphingolipids concentrate in the inner invaginations of the multivesicular body (Sandhoff and Klein, 1994). Interestingly, a unique lipid, lyso-bisphosphatic acid, also has been found to associate with these inner invaginations and the latter stages of the endocytic pathway (Kobayashi *et al.*, 1998), suggesting that the biophysical properties of the lipids influence their trafficking in this pathway. If this property were also important for the membrane proteins, then fluidity considerations alone could account for the loss of recycling efficiency, with the larger TR complexes being trapped in the multivesicular body through losses in lateral mobility. Clearly, there is evidence that the diffusion coefficients of membrane proteins are higher in tubular extensions than in larger structures (Berk and Hochmuth, 1992). This is also consistent with the idea that differences in lipid composition affect membrane protein trafficking.

Because our model suggests that polar residues in the TM promote down-regulation of the TR complexes, we examined other TR TM sequences to confirm the absence of polar residues, especially in the region of interest, residues 11–19. As can be seen in Table 1, polar residues are lacking within this region in all the TR sequences identified. Interesting, this lack of polar residues appears to also be true for the low-density lipoprotein as well, another transport receptor that efficiently recycles. However, when we examined the TM sequences for other cell surface proteins that have an unusual number of polar residues, we find an interesting ensemble of proteins that traffic to late endosomal/lysosomal compartments (Table 2). This implies that TM polar residues may represent a common, mechanistically simple way to sort membrane proteins in the endocytic pathway without the specific need of a cytoplasmic tail "lysosomal targeting signal." It is interesting that one of the proteins identified in the search, P-selectin, was also a protein in which a cytoplasmic tail lysosomal targeting signal was

difficult to localize (Straley *et al.*, 1998). And finally in support of our proposed model, it is now clear that receptor down-regulation requires multiple rounds of recycling before lysosomal delivery occurs (Lai *et al.*, 1989; Felder *et al.*, 1992), suggesting that down-regulation, rather than being a distinctive all-or-nothing event, may simply reflect a loss of recycling fidelity (Weissman *et al.*, 1986).

To correlate loss of recycling efficiency with protein half-life, we developed a mathematical model for recycling in the endocytic pathway (see MATERIALS AND METHODS for details of the calculation). In this model, membrane proteins in the recycling pathway are found at the plasma membrane or the endosome or between these compartments. For sake of simplicity, we considered the plasma membrane and sorting endosome as one compartment and the lysosome as a second compartment. The protein half-life ($t_{1/2}$) is defined as the period of time required for recycling (p) multiplied by the ln of 0.5 divided by the ln of the recycling efficiency (λ). Because the half-life determination also requires that the newly synthesized protein be delivered to the cell surface, this transit time to the surface (t_{sur}) must be added to this equation as well. From this,

$$t_{1/2} = \frac{p\ln(0.5)}{\ln(\lambda)} + t_{sur} \qquad (13)$$

simple model, if the transit time is 1 h and the recycling time is <1 h (~40 min), it is clear that as recycling efficiency approaches 100%, the protein half-life is influenced dramatically. For example, if the recycling efficiency is 98%, then the protein half-life estimates from this calculation would be 23.9 h (Table 3). If however, the recycling efficiency decreases to 92%, the calculated half-life is 6.5 h, which agrees well with the experimentally determined half-life of 5.6 h (Table 3).

Our results suggest that protein down-regulation is not an efficient process per single round of endocytosis and recycling, but because the cycle occurs repeatedly, efficient clearance of surface proteins occurs with even small losses in recycling efficiency. Down-regulation of most proteins usually occurs over several hours, suggesting that a partial loss of recycling efficiency would be all that was necessary to explain down-regulation for most proteins. This also suggests that lysosomal targeting, at least from the cell surface, may not require specific cytoplasmic tail sorting signals for efficient delivery, but may reflect the biophysical properties of the proteins themselves in the sorting endosome. Protein sorting in the sorting endosome based on fluidity consider-

ations alone would explain the lack of progress at identifying coat proteins at this site. Clearly, segregation of proteins occurs in the sorting endosome, and based on the studies presented herein, we propose that segregation of recycling and down-regulated receptors can be accomplished without the need of a specific cytoplasmic tail sorting determinant.

Note added in proof. A recent study by J.B. Ashman and J. Miller (J. Immunol. [1999]. *163*:2704–2712) demonstrated that polar residues in the murine invariant chain are important for trimerization. This, coupled with our studies, suggests that the orientation of the polar residues within transmembrane domains can influence both subunit assembly and aggregation status. Interestingly, in the mouse sequence, position 11 has an alanine rather than a threonine, making difficult the burying of all the polar residues at subunit contact sites in the human invariant chain transmembrane domain, even in the context of a trimer. Our study agrees with theirs in that protein associations occur through polar residues in the transmembrane domain.

ACKNOWLEDGMENTS

REFERENCES

Alvarez, E., Girones, N., and Davis, R.J. (1989). Intermolecular disulfide bonds are not required for the expression of the dimeric state and functional activity of the transferrin receptor. EMBO J. *8*, 2231–2240.

Bakke, O., and Dobberstein, B. (1990). MHC class II-associated invariant chain contains a sorting signal for endosomal compartments. Cell *63*, 707–716.

Berk, D.A., and Hochmuth, R.M. (1992). Analysis of lateral diffusion from a spherical cell surface to a tubular projection. Biophys. J. *61*, 1–8.

Bo, L., Quarles, R.H., Fujita, N., Bartoszewicz, Z., Sato, S., and Trapp, B.D. (1995). Endocytic depletion of L-MAG from CNS myelin in quaking mice. J. Cell Biol. *131*, 1811–1820.

Bradbury, L.E., Goldmacher, V.S., and Tedder, T.F. (1993). The CD19 signal transduction complex of B lymphocytes. J. Immunol. *151*, 2915–2927.

Bremnes, B., Madsen, T., Gedde-Dahl, M., and Bakke, O. (1994). An LI and ML motif in the cytoplasmic tail of the MHC-associated invariant chain mediate rapid internalization. J. Cell Sci. *107*, 2021–2032.

Carpenter, G., and Cohen, S. (1976). 125I-labeled human epidermal growth factor. Binding, internalization, and degradation in human fibroblasts. J. Cell Biol. *71*, 159–171.

Carson, M. (1997). Ribbons. Methods Enzymol. *277*, 493–505.

Collawn, J.F., Lai, A., Domingo, D., Fitch, M., Hatton, S., and Trowbridge, I.S. (1993). YTRF is the conserved internalization signal of the transferrin receptor, and a second YTRF signal at position 31–34 enhances endocytosis. J. Biol. Chem. *268*, 21686–21692.

Dautry-Varsat, A., Ciechanover, A., and Lodish, H.F. (1983). pH and the recycling of transferrin during receptor-mediated endocytosis. Proc. Natl. Acad. Sci. USA *80*, 2258–2262.

Diaz, E., and Pfeffer, S.R. (1998). TIP47: a cargo selection device for mannose 6-phosphate receptor trafficking. Cell *93*, 433–443.

Dunn, W.A., Connolly, T.P., and Hubbard, A.L. (1986). Receptor-mediated endocytosis of epidermal growth factor by rat hepatocytes: receptor pathway. J. Cell Biol. *102*, 24–36.

Felder, S., LaVin, J., Ullrich, A., and Schlessinger, J. (1992). Kinetics of binding, endocytosis, and recycling of EGF receptor mutants. J. Cell Biol. *117*, 203–212.

Fuchs, H., Lucken, U., Tauber, R., Engel, A., and Gessner, R. (1998). Structural model of phospholipid-reconstituted human transferrin receptor derived by electron microscopy. Structure *6*, 1235–1243.

Futter, C.E., Felder, S., Schlessinger, J., Ullrich, A., and Hopkins, C.R. (1993). Annexin I is phosphorylated in the multivesicular body during the processing of the epidermal growth factor receptor. J. Cell Biol. *120*, 77–83.

Gerhardt, E.M., Chan, L.-N.L., Jing, S., Qi, M., and Trowbridge, I.S. (1991). The cDNA sequence and primary structure of the chicken transferrin receptor. Gene *102*, 249–254.

Graeve, L., Drickamer, K., and Rodriguez-Boulan, E. (1989). Polarized endocytosis by Madin-Darby canine kidney cells transfected with functional chicken liver glycoprotein receptor. J. Cell Biol. *109*, 2809–2816.

Green, S.A., Setiadi, H., McEver, R.P., and Kelly, R.B. (1994). The cytoplasmic domain of P-selectin contains a sorting determinant that mediates rapid degradation in lysosomes. J. Cell Biol. *124*, 435–448.

Gruenberg, J., and Maxfield, F.R. (1995). Membrane transport in the endocytic pathway. Curr. Opin. Cell Biol. *7*, 552–563.

Hansen, J.C., Lebowitz, J., and Demeler, B. (1994). Analytical ultracentrifugation of complex macromolecular systems. Biochemistry *33*, 13155–13163.

Hopkins, C.R. (1983). Intracellular routing of transferrin and transferrin receptors in epidermoid carcinoma A431 cells. Cell *35*, 321–330.

Hughes, S.H., Petropoulos, C.J., Federspiel, M.J., Sutrave, P., Forry-Schaudies, S., and Bradac, J.A. (1990). Vectors and genes for improvement of animal strains. J. Reprod. Fert. Suppl. *41*, 39–49.

Jiang, W., Swiggard, W.J., Heufler, C., Peng, M., Mirza, A., Steinman, R.M., and Nussenzweig, M.C. (1995). The receptor DEC-205 expressed by dendritic cells and thymic epithelial cells is involved in antigen processing. Nature *375*, 151–155.

Jing, S., Spencer, T., Miller, K., Hopkins, C., and Trowbridge, I.S. (1990). Role of the human transferrin receptor cytoplasmic domain in endocytosis: localization of a specific signal sequence for internalization. J. Cell Biol. *110*, 283–294.

Jing, S., and Trowbridge, I.S. (1987). Identification of the intermolecular disulfide bonds of the human transferrin receptor and its lipid-attachment site. EMBO J. *6*, 327–331.

Johnson, K.F., and Kornfeld, S. (1992a). The cytoplasmic tail of the mannose 6-phosphate/insulin-like growth factor-II receptor has two signals for lysosomal enzyme sorting in the golgi. J. Cell Biol. *119*, 249–257.

Johnson, K.F., and Kornfeld, S. (1992b). A his-leu-leu sequence near the carboxyl terminus of the cytoplasmic domain of the cation-dependent mannose 6-phosphate receptor is necessary for the lysosomal enzyme sorting function. J. Biol. Chem. *267*, 17110–17115.

Johnson, L.S., Dunn, K.W., Pytowski, B., and McGraw, T.E. (1993). Endosome acidification and receptor trafficking: bafilomycin A1 slows receptor externalization by a mechanism involving the receptor's internalization motif. Mol. Biol. Cell *4*, 1251–1266.

Kang, S., Liang, L., Parker, C.D., and Collawn, J.F. (1998). Structural requirements for major histocompatibility complex class II invariant chain endocytosis and lysosomal targeting. J. Biol. Chem. *273*, 20644–20652.

Klausner, R.D., Ashwell, G., van Renswoude, J., Harford, J.E., and Bridges, K.R. (1983). Binding of apotransferrin to K562 cells: explanation of the transferrin cycle. Proc. Natl. Acad. Sci. USA *80*, 2263–2266.

Kobayashi, T., Stang, E., Fang, K.S., de Moerloose, P., Parton, R.G., and Gruenberg, J. (1998). A lipid associated with the antiphospholipid syndrome regulates endosome structure and function. Nature *392*, 193–197.

Kunkel, T.A. (1985). Rapid and efficient site-specific mutagenesis without phenotypic selection. Proc. Natl. Acad. Sci. USA *82*, 488–492.

Lai, W.H., Cameron, P.H., Wada, I., Doherty, J.J., Kay, D.G., Posner, B.I., and Bergeron, J.J. (1989). Ligand-mediated internalization, recycling, and down regulation of the epidermal growth factor receptor in vivo. J. Cell Biol. *109*, 2741–2749.

Letourneur, F., and Klausner, R.D. (1992). A novel di-leucine motif and a tyrosine-based motif independently mediate lysosomal targeting and endocytosis of CD3 chains. Cell *69*, 1143–1157.

Lippincott-Schwartz, J., and Fambrough, D.M. (1986). Lysosomal membrane dynamics: structure and interorganellar movement of a major lysosomal membrane glycoprotein. J. Cell Biol. *102*, 1593–1605.

Lippincott-Schwartz, J., and Fambrough, D.M. (1987). Cycling of the integral membrane glycoprotein, LEP100, between plasma membrane and lysosomes: kinetic and morphological analysis. Cell *49*, 669–677.

Marsh, E.W., Leopold, P.L., Jones, N.L., and Maxfield, F.R. (1995). Oligomerized transferrin receptors are selectively retained by a lumenal sorting signal in a long-lived endocytic recycling compartment. J. Cell Biol. *129*, 1509–1522.

Martin, R.G., and Ames, B.N. (1961). A method for determining the sedimentation behavior of enzymes: application to protein mixtures. J. Biol. Chem. *236*, 1372–1379.

Mayor, S., Presley, J.F., and Maxfield, F.R. (1993). Sorting of membrane components from endosomes and subsequent recycling to the cell surface occurs by a bulk flow process. J. Cell Biol. *121*, 1257–1269.

McClelland, A., Kuhn, L.C., and Ruddle, F.H. (1984). The human transferrin receptor gene: genomic organization, and the complete primary structure of the receptor deduced from a cDNA sequence. Cell *39*, 267–274.

Mellman, I. (1996). Endocytosis and molecular sorting. Annu. Rev. Cell. Dev. Biol. *12*, 575–625.

Mellman, I., and Plutner, H. (1984). Internalization and degradation of macrophage Fc receptors bound to polyvalent immune complexes. J. Cell Biol. *98*, 1170–1177.

Mellow, T.E., Halberg, D., and Drickamer, K. (1988). Endocytosis of N-acetylglucosamine-containing glycoproteins by rat fibroblasts expressing a single species of chicken liver glycoprotein receptor. J. Biol. Chem. *263*, 5468–5473.

Mukherjee, S., Ghosh, R.N., and Maxfield, F.R. (1997). Endocytosis. Physiol. Rev. *77*, 759–803.

Mukherjee, S., Soe, T.T., and Maxfield, F.R. (1999). Endocytic sorting of lipid analogues differing solely in the chemistry of their hydrophobic tails. J. Cell Biol. *144*, 1271–1284.

Odorizzi, C.G., Trowbridge, I.S., Xue, L., Hopkins, C.R., Davis, C.D., and Collawn, J.F. (1994). Sorting signals in the MHC class II invariant chain cytoplasmic tail and transmembrane region determine trafficking to an endocytic processing compartment. J. Cell Biol. *126*, 317–330.

Oka, Y., Rozek, L.M., and Czech, M.P. (1985). Direct demonstration of rapid insulin-like growth factor II receptor internalization and recycling in rat adipocytes. Insulin stimulates ^{125}I-insulin-like growth factor II degradation by modulating the IGF-II receptor recycling process. J. Biol. Chem. *260*, 9435–9442.

Omary, M.B., and Trowbridge, I.S. (1981). Biosynthesis of the human transferrin receptor in cultured cells. J. Biol. Chem. *256*, 12888–12892.

Peters, C., Braun, M., Weber, B., Wendland, M., Schmidt, B., Pohlmann, R., Waheed, A., and von Figura, K. (1990). Targeting of a lysosomal membrane protein: a tyrosine-containing endocytosis signal in the cytoplasmic tail of lysosomal acid phosphatase is necessary and sufficient for targeting to lysosomes. EMBO J. *9*, 3497–3506.

Pieters, J., Bakke, O., and Dobberstein, B. (1993). The MHC class II-associated invariant chain contains two endosomal targeting signals within its cytoplasmic tail. J. Cell Sci. *106*, 831–846.

Pond, L., Kuhn, L.A., Teyton, L., Schutze, M.-P., Tainer, J.A., Jackson, M.R., and Peterson, P.A. (1995). A role for acidic residues in di-leucine motif-based targeting to the endocytic pathway. Biol. Chem. *270*, 19989–19997.

Rutledge, E.A., Mikoryak, C.A., and Draper, R.K. (1991). Turnover of the transferrin receptor is not influenced by removing most of the extracellular domain. J. Biol. Chem. *266*, 21125–21130.

Sandhoff, K., and Klein, A. (1994). Intracellular trafficking of glycosphingolipids: role of sphingolipid activator proteins in the topology of endocytosis and lysosomal digestion. FEBS Lett. *346*, 103–107.

Sanger, F., Nicklen, S., and Coulson, R. (1977). DNA sequencing with chain-terminating inhibitors. Proc. Natl. Acad. Sci. USA *74*, 5463–5467.

Solari, R., Smithers, N., Kennard, N., Ray, K., and Grenfell, S. (1994). Receptor mediated endocytosis and intracellular fate of IL-1. Biochem. Pharmcol. *47*, 93–101.

Sorokin, A., Mohammadi, M., Huang, J., and Schlessinger, J. (1994). Internalization of fibroblast growth factor receptor is inhibited by a point mutation at tyrosine 766. J. Biol. Chem. *269*, 17056–17061.

Straley, K.S., Daugherty, B.L., Aeder, S.E., Hockenson, A.L., Kim, K., and Green, S.A. (1998). An atypical sorting determinant in the cytoplasmic domain of P-selectin mediates endosomal sorting. Mol. Biol. Cell *9*, 1683–1694.

Tabor, S., and Richardson, C.C. (1987). DNA sequence analysis with a modified bacteriophage T7 DNA polymerase. Biochemistry *84*, 4767–4771.

Trowbridge, I.S., Domingo, D.L., Thomas, M.L., and Chain, A. (1988). Cell surface molecules of the hematopoietic system: T200 glycoprotein and the transferrin receptor as models for proteins involved in growth and differentiation. In: Inflammatory Bowel Disease: Current Status and Future Approach, Amsterdam: Elsevier Publishing Co., 441–447.

Turkewitz, A.P., Schwartz, A.L., and Harrison, S.C. (1988). A pH-dependent reversible conformational transition of the human transferrin receptor leads to self-association. J. Biol. Chem. *263*, 16309–16315.

Weissman, A.M., Klausner, R.D., Rao, K., and Harford, J.B. (1986). Exposure of K562 cells to anti-receptor monoclonal antibody OKT9 results in rapid redistribution and enhanced degradation of the transferrin receptor. J. Cell Biol. *102*, 951–958.

Weisz, O.A., Swift, A.M., and Machamer, C.E. (1993). Oligomerization of a membrane protein correlates with its retention in the Golgi complex. J. Cell Biol. *122*, 1185–1196.

Wileman, T.E., Lennartz, M.R., and Stahl, P.D. (1986). Identification of the macrophage mannose receptor as a 175-kDa membrane protein. Proc. Natl. Acad. Sci. USA *83*, 2501–2505.

Wiley, H.S., and Cunningham, D.D. (1982). The endocytotic rate constant: a cellular parameter for quantitating receptor-mediated endocytosis. J. Biol. Chem. *257*, 4222–4229.

Williams, M.A., and Fukuda, M. (1990). Accumulation of membrane glycoproteins in lysosomes requires a tyrosine residue at a particular position in the cytoplasmic tail. J. Cell Biol. *111*, 955–956.

Willingham, M.C., Hanover, J.A., Dickson, R.B., and Pastan, I. (1984). Morphologic characterization of the pathway of transferrin endocytosis and recycling in human KB cells. Proc. Natl. Acad. Sci. USA *81*, 175–179.

Yellin, M.J., Sippel, K., Inghirami, G., Covey, L.R., Lee, J.J., Sinning, J., Clark, E.A., Chess, L., and Lederman, S. (1994). CD40 molecules induce down-modulation and endocytosis of T cell surface T cell-B cell activating molecule/CD40-L. Potential role in regulating helper effector function. J. Immunol. *152*, 598–608.